MODELLING OF THE IGNITION INSIDE A TURBOJET COMBUSTOR. APPLICATION TO IN-FLIGHT RELIGHT.

Nawel OUARTI, Gérard LAVERGNE, Renaud LECOURT

ONERA/DMAE/MH
2 Avenue Edouard Belin, BP 4025
31055 Toulouse Cedex 4, FRANCE
Phone : 33 (0)5 62 25 25 25 #24 34
Fax : 33 (0)5 62 25 25 83
E-mail : Nawel.Ouarti@onecert.fr

ABSTRACT

At high altitude, the operating critical conditions make the ignition and the relighting of jet engine combustors more difficult to control. The objective of ONERA is to develop a computational tool to predict ignition inside the turbojet combustor, according to the internal two-phase flow field and the igniter's location. To study the flame kernel initiation, a one-dimensional model has been developed to predict the ignition of a spherical two-phase kernel when submitted to the electrical spark. To study the flame kernel propagation, the kernel's ignition model is then coupled with the ONERA's CEDRE code, to follow the kernel's evolution and finally conclude on the flame's extinction or on the chamber's ignition. Experiments were performed on a combustion chamber of simple geometry to test ignition at ambient temperature under atmospheric pressure and under low pressure. A high-speed intensified video camera provided characterisations of the complete ignition phenomenon. The turbulent two-phase flow field corresponding to the experimental combustor and the complete ignition process within were computed and provided numerical results that are in good agreement with the experimental ones. In the paper, the numerical model is presented in detail, and some examples of its application to the experimental configuration are discussed.

INTRODUCTION

The ignition performance of a turbojet engine is usually characterised by the operating range in terms of altitude over which ignition is feasible or can be re-established after an accidental in-flight flameout. At high altitude, the adverse climatic conditions of low pressure and low temperature sharply limit the concentration of fuel vapour available in the vicinity of the igniter plug, by the effect of low volatility on evaporation rate, and by the effect of high viscosity on mean fuel-drops size.

The objective of ONERA (French Aeronautics and Space Research Centre), in collaboration with ADEME (French Agency for Environment and Energy Management) is to develop a numerical tool to predict ignition in the turbojet combustor, according to the internal two-phase flow field and the igniter's location, in order to help the design of practical devices.

For gas turbines the most satisfactory and convenient mode of ignition is the electrical spark's discharge that converts the electrical energy fairly efficiently into heat concentrated in a relatively small volume.
Then three phases should be distinguished to complete the ignition process (Fig.1) :

✔ the ignition, resulting from the spark's discharge, of a flame kernel that must be of sufficient size and temperature level to be able to propagate;

✔ the flame's propagation to the primary zone of the combustion chamber;

✔ the ignition's propagation to the whole chamber.

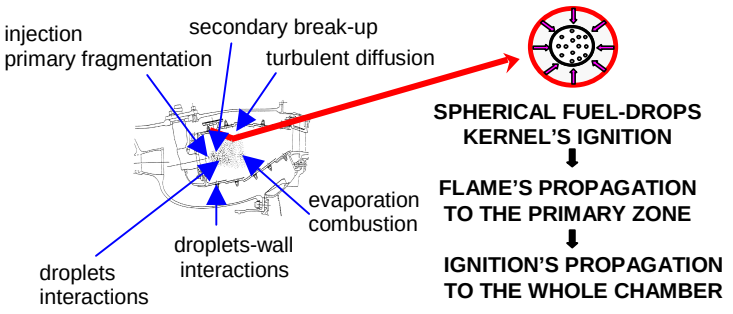

Fig. 1 : Ignition process inside a turbojet combustion chamber

MODELLING APPROACH

First step

The turbulent two-phase flow field within the combustion chamber is computed with the ONERA's CEDRE code using an Eulerian-Lagrangian approach, in two-way coupling.
The gas flow field is simulated by solving the averaged Navier-Stokes equations with a k-l_m formulation to describe turbulence. The implicit resolution is performed with a finite volume scheme.

To compute the discrete phase, a stochastic Lagrangian method is used to track the particles. Each numerical drop represents a large number of real droplets. Several classes of drops are defined according to their diameters, their injection points, and their velocities. Once injected into the combustion chamber, the drops are transported by the gas flow, dispersed by the turbulent structures, evaporated, and may interact with a wall (rebound, streaming). To determine the particle's trajectory, a second order Runge-Kutta method is used to solve the fuel-drop equation of motion.

Second step

Once defined the kernel on which ignition will be tested, the injection of energy has to be modelled.
The spark's discharge creates a pressure wave when the kernel expands in volume. Nevertheless this pressure perturbation propagates with the local sound celerity so it moves away fast enough to assume the ignition process to be isobaric : in a kernel of 3mm radius, considering a local sound velocity of 300m/s, the pressure perturbation moves away in 10^{-5}s from the ignition zone which is negligible in comparison with the characteristic kernel's ignition delay included between 0.1 and 1ms.
The energy delivered by the spark generates at the same time the heating and the expansion of the kernel.

Kernel's heating. The spatial distribution of the energy delivered by the spark's discharge has to be taken into account, as suggested by A.Dreizler and al. [1] that plan a spatial exponential decrease of the energy injected.

Kernel's dilatation. The state equation of the gas allows to estimate the kernel's radius after the spark's discharge.

Then, knowing the conditions of pressure, temperature, and turbulence, as well as the drops distribution within the expanded kernel, thanks to the previous two-phase flow field computation, the kernel's ignition model may be applied.

Third Step

The kernel's ignition is successful if the rate of heat release by combustion exceeds the turbulent losses outside the kernel; if the temperature inside the kernel increases significantly after the spark's discharge and if combustion products are actually created, the kernel's ignition may be considered as effective.

Then, the kernel's ignition model is coupled with the ONERA's CEDRE code providing the data necessary to the computation of the kernel's transportation, such as the temperature level, the species mass fractions, and the droplets distribution within the expanded kernel. The last computation is conducted in two-way coupling, in reactive mode, with a turbulent combustion model. The evolution of the temperature level inside the combustion chamber, as well as the evolution of the combustion products mass fraction allow to conclude on the combustor's ignition.

KERNEL'S IGNITION MODEL

The fuel-drops kernel's ignition model (Fig.2) is based on the following assumptions :

✔ The outer temperature and pressure are fixed as boundary conditions.

✔ The liquid phase is entirely composed of a mono-component fuel (n-decane).

✔ The drops are evenly distributed within the spherical kernel, characterised by a constant density per volume unit *n*.

✔ During its ignition, the kernel is supposed to be motionless, as well as the fuel-drops : this assumption may be justified by comparing the displacement of the kernel during the ignition process with the kernel's radius.

✔ Drops interactions are neglected.

✔ The gas satisfies the state equation for real gas.

✔ The laminar mass diffusion coefficient is negligible compared with the turbulent one :

$D = D_l + D_t$, with $D_l << D_t$, that is $D \approx D_t$

✔ The turbulent Lewis number is assumed to be equal to unity :

$$Le_t = \frac{\lambda_t}{\rho C_p D_t} = 1 \qquad \lambda_t = \rho C_p D_t$$

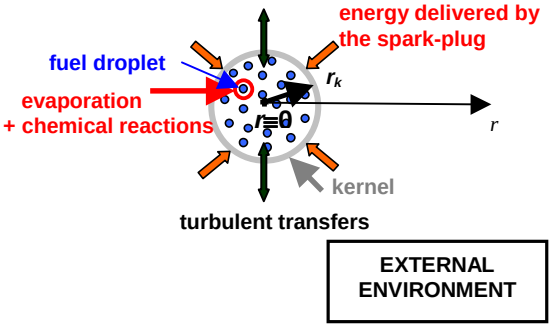

Fig. 2 : Schematic representation of the spherical ignition kernel

Under these assumptions, the governing equations (Equations (1) through (6)) for the kernel's ignition model can be written; they form a system of one-dimensional, time-dependent equations, expressing the mass species conservation, the energy conservation, and the state equation for the gas (the compressibility factor *Z* takes account of the gas dissociation at high temperature).

By means of source terms, this system takes account of the different physical phenomena involved, such as :

✔ the fuel-drops evaporation, using the infinite conduction model of Abramzon and Sirignano [2], which assumes that heat conduction inside the liquid droplet occurs infinitely fast regarding the mass and heat exchange phenomena;

✔ the chemical kinetics, governed by a one-step global and irreversible reaction : ν_F Fuel + ν_{Ox} Ox → ν_P Prod;

The rate of reaction is expressed by the Arrhenius law, using the parameters to describe the n-decane oxidation recommended by Westbrook and Dryer [3].

✔ the turbulent transfers, assumed to occur at the interface between the kernel and its surroundings in a thermal and diffusion film whose thickness is equal to the turbulence length scale l_m.

$$\rho \frac{\partial Y_F}{\partial t} - \frac{D_t}{r^2}\frac{\partial}{\partial r}\left(\rho r^2 \frac{\partial Y_F}{\partial r}\right) = \dot{n}\dot{m}(1 - Y_F) - \nu_F W_F \dot{\omega} \quad (1)$$

$$\rho \frac{\partial Y_O}{\partial t} - \frac{D_t}{r^2}\frac{\partial}{\partial r}\left(\rho r^2 \frac{\partial Y_O}{\partial r}\right) = -\dot{n}\dot{m} Y_O - \nu_O W_O \dot{\omega} \quad (2)$$

$$\rho \frac{\partial Y_P}{\partial t} - \frac{D_t}{r^2}\frac{\partial}{\partial r}\left(\rho r^2 \frac{\partial Y_P}{\partial r}\right) = -\dot{n}\dot{m} Y_P + \nu_P W_P \dot{\omega} \quad (3)$$

$$\rho \frac{\partial Y_{N_2}}{\partial t} - \frac{D_t}{r^2}\frac{\partial}{\partial r}\left(\rho r^2 \frac{\partial Y_{N_2}}{\partial r}\right) = -\dot{n}\dot{m} Y_{N_2} \quad (4)$$

$$\frac{\partial T}{\partial t} - \frac{D_t}{\rho r^2}\frac{\partial}{\partial r}\left(\rho r^2 \frac{\partial T}{\partial r}\right) = \frac{1}{\rho C_p(T)} \times -\dot{n}\dot{m}\frac{1 + B_T}{B_T}\left[C_{pv}(T_{ref})(T - T_s) + \nu_F W_F \dot{\omega} Q_c\right] \quad (5)$$

$$P = Z\rho r_{gp} T = Z\rho R_{gp} \sum_k \frac{Y_k}{W_k}\Big|T = P_\infty = constant \quad (6)$$

§ Unknown quantities : (ρ, Y_k, T)

§ Boundary conditions : $r = 0$: $\frac{\partial Y_k}{\partial r} = 0$ and $\frac{\partial T}{\partial r} = 0$; $r \infty$: $Y_k = Y_{k\infty}$ and $T = T_\infty$

§ Initial conditions : $t = 0$: $Y_k = Y_{k0}$; $T = T_0$; $\rho = \rho_0 = \frac{P_0}{Z_0 r T_0}$

The system is solved using an explicit method : the central finite difference scheme is adopted for spatial derivatives while the forward finite difference scheme for time derivatives.

EXPERIMENTAL STUDY

Tests were carried out on an experimental set-up composed of an air supply, a plenum chamber, an airblast injector, a turbojet engine spark-plug and a parallelepipedic combustion chamber equipped with a porthole (Fig.3).

The instrumentation associated with the set-up is composed of two flow-meters to measure the kerosene and the air mass flow rates, two thermocouples to determine the kerosene and the air injection temperatures, and a differential pressure transducer to estimate the air pressure drop across the injection system.

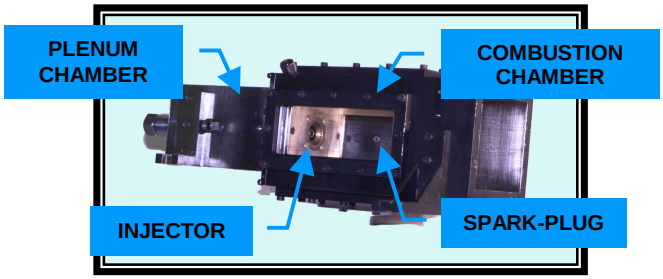

Fig. 3 : Experimental set-up

All the experiments have been carried out at ambient temperature (T=288K), first under atmospheric pressure (P=1bar) and next under low pressure (P=0.55bar). Five spark-plug's locations were tested (27.5, 57.5, 87.5, 117.5 and 147.5mm far from the injection face at mid-height of the combustion chamber).

The experimental procedure was defined as follow : first, air is injected during about 20s to adjust the injection pressure drop. Then, air and kerosene are injected simultaneously during 3s, while the spark-plug is discharging at a frequency of 3Hz, producing 9 to 10 sparks to allow ignition.

Tests under atmospheric pressure

Figure 4 presents the success and failures of the ignition tests at atmospheric pressure, for each spark-plug location, in a "reduced mass flow rate / equivalence ratio" diagram.

The two first spark-plug's locations appear as the most favourable to obtain the complete ignition of the combustion chamber.

The locations more far away from the injector allow ignition only for an equivalence ratio greater than 2.

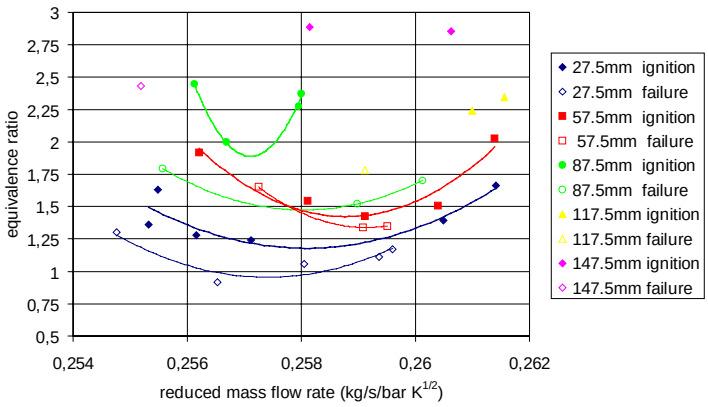

Fig. 4 : Ignition domain

When ignition occurred, black and white pictures were taken with the high-speed intensified video camera used in the visible range at a rate of 1000fps. To obtain a complete view of the phenomenon, lateral and frontal visualisations have been successively carried out for each operating point. Figure 5 presents the ignition sequence for an operating point characterised by an equivalence ratio close to 1.9 and a reduced mass flow rate of about 0.26, for the spark-plug located at 57.5mm far from the injector. On the lateral views (Fig.5a), four steps can be distinguished concerning the ignition scenario. First of all, a combustion zone is created after the spark's discharge. Then, this zone seems to disappear. In a third step, several burning zones develop next to the initial ignited kernel. Finally, the burning zones merge together in a large single zone, whose size increases quickly to fill the whole combustion chamber. The frontal visualisations (Fig.5b) add new information about the ignition process : after the spark's discharge, the burning zone moves slowly towards the top of the chamber; next this zone grows, winding round the chamber's axis because of the swirling flow generated by the injection system.

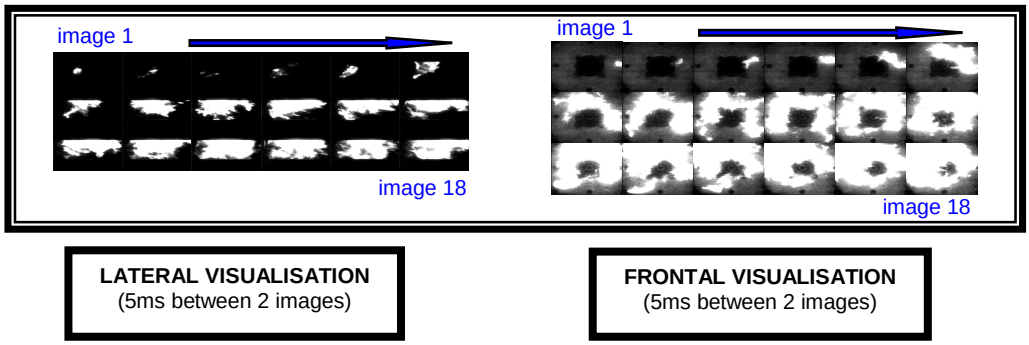

(a) **(b)**

Fig. 5 : Lateral and frontal visualisations of ignition

Tests under low pressure

A second combustion chamber was added in extension to the first one and a suction system was set up to ensure an average chamber's pressure of about 0.55bar. Only the two first spark-plug's locations were tested. Even in the most favourable operating conditions, a stabilised ignition could not be established. A low air flow rate seems to facilitate the ignition starting.

TWO-PHASE FLOW AND IGNITION SIMULATION

Two-phase flow field computation

Because of the swirling flow generated by the airblast injector, the computational mesh is chosen two-dimensional and axisymmetric. Ten injection points are defined according to an even distribution along the vertical axis close to the exit of the airblast injector. The mean fuel-drops sizes and velocities have been determined previously by PDPA characterisations of the spray produced by the injection system; then four sizes classes are defined respecting the experimental Sauter Mean Diameter of about 65µm.

The two-phase flow field within the combustion chamber was computed using the ONERA's CEDRE code under ambient temperature (T=288K) and atmospheric pressure (P=1bar), in two-way coupling (Fig.6).

The central recirculation zone is characteristic of the airblast injector that generates a swirling flow thanks to a spins system. Two other recirculation zones also appear in the periphery of the chamber's axis.

Part of the smallest droplets are trapped by the axial and lateral recirculation zones while part of these droplets and the intermediate size droplets extract themselves from the recirculation zones. The biggest droplets are not influenced by the gas flow and follow the trajectory resulting from the injection conditions.

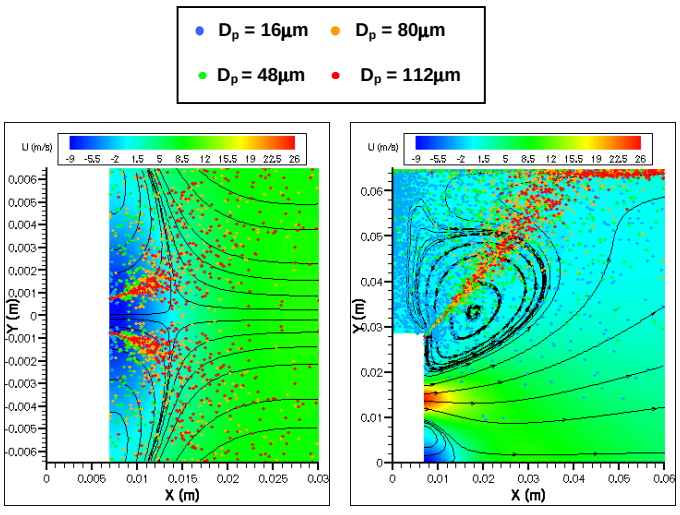

(a) **(b)**

Fig.6 : Superimposition of the axial velocity field of the gas and the trajectories of the injected droplets :
(a) near the combustor's axis
(b) in the peripheral recirculation zone

Kernel's ignition

Tests were carried out to determine the performance of the spark-plug used under the experimental bench. They confirmed the spark's duration (of about 40µs) announced by the manufacturer and allowed to evaluate the size of the lighted zone when the spark-plug discharges (of about 3mm radius); this size is then considered as the initial ignition kernel's size.

The kernel's ignition tests were performed for the spark-plug located at 57.5mm far from the injector, for two different injected equivalence ratios, respectively equal to 1.25 and 1.75, as suggested by the ignition domain (Fig.4). Figure 7 presents the evolutions of temperature and species mass fractions inside the kernel for the two studied cases. The spark's discharge generates a violent increase in temperature. The fuel evaporates and reacts with the oxygen to create the combustion products. The runaway of the chemical reactions is underlined by the consumption of fuel and oxygen on the one hand and by the creation of combustion products on the other hand. The ignition phase is characterised by a new increase in temperature inside the kernel. Next, the products mass fraction decreases because of the species diffusion and the oxygen mass fraction increases because of the new supply in oxygen coming from outer environment. At the same time, the temperature decreases under the heat diffusion effect.

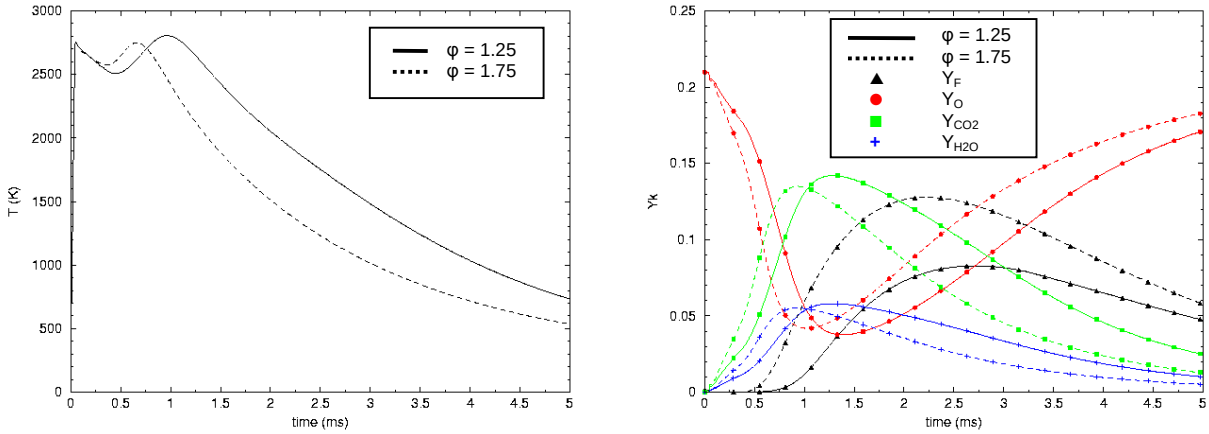

Fig. 7 : Temporal evolutions of temperature and species mass fractions inside the kernel

In both cases, the kernel's ignition is effective so the computation of the kernel's transportation is necessary to differentiate these two configurations to finally conclude on the effective ignition of the whole combustor.

Combustor's ignition

Figures 8 and 9 present the evolution of the temperature inside the combustor, once the kernel is ignited. For an injected equivalence ratio equal to 1.25, the ignited kernel vanishes quickly, in about ten milliseconds. On the contrary, for an injected equivalence ratio equal to 1.75, the ignited kernel is convected and diffused, and finally the flame propagates to the whole chamber, in a delay of about forty milliseconds.

These results are in accordance with the experimental ones, summarised on Figure 4, first in a global way about ignition or extinction of the combustion chamber, and next about the ignition delay in the case of the flame's propagation.

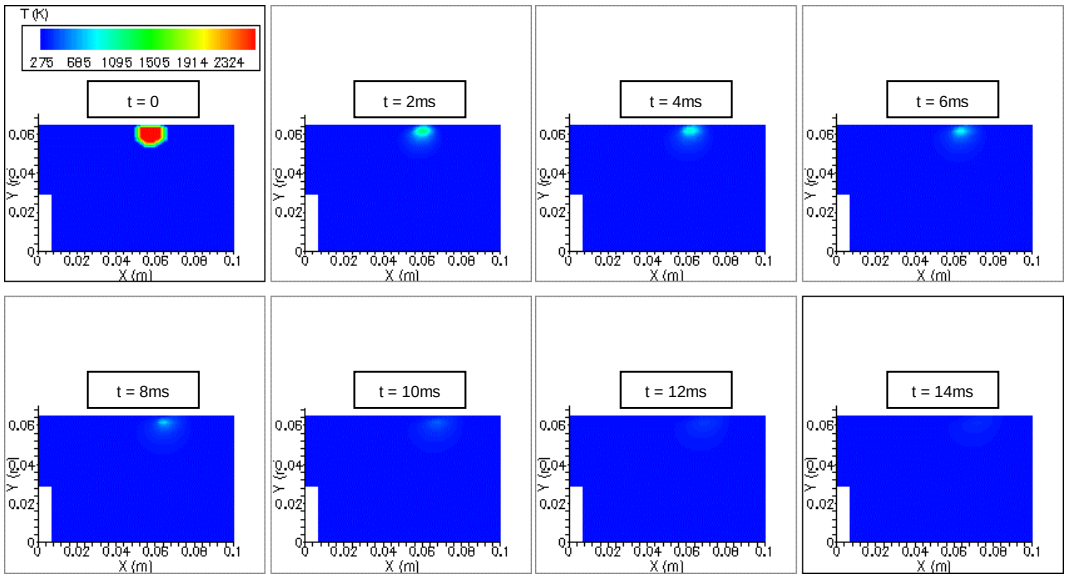

Fig. 8 : Temporal evolution of temperature inside the combustor after kernel's ignition (φ = 1.25)

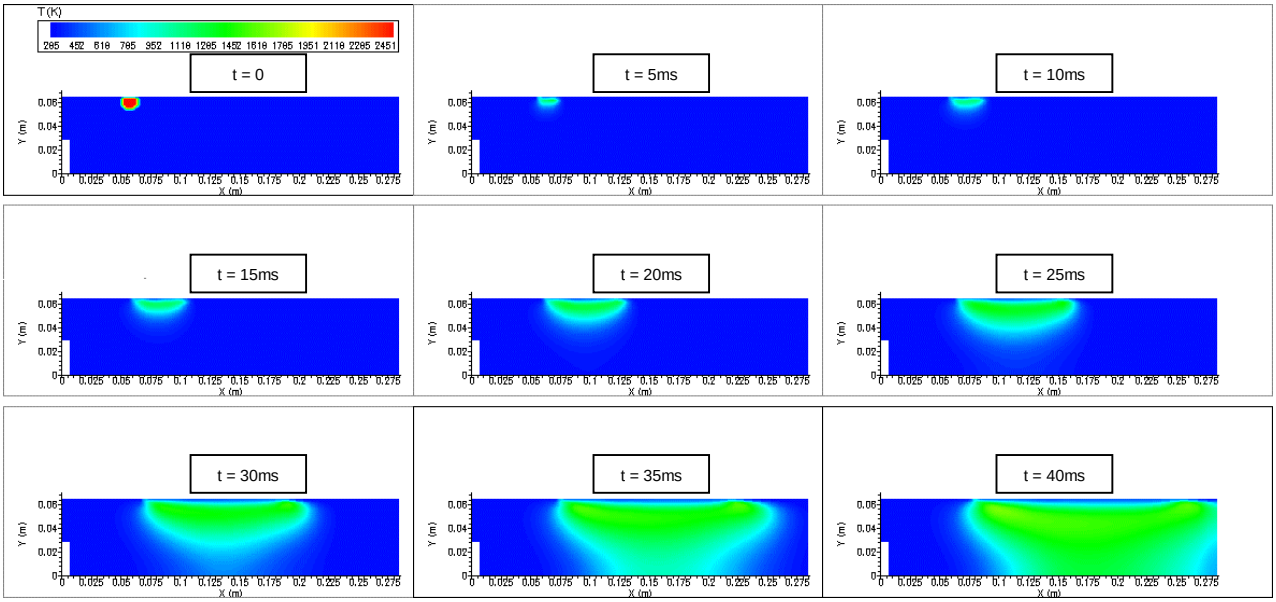

Fig. 9 : Temporal evolution of temperature inside the combustor after kernel's ignition (φ = 1.75)

CONCLUSION AND PERSPECTIVES

A numerical model predicting the ignition of a two-phase kernel containing fuel-drops and submitted to the spark's discharge inside the combustion chamber has been developed and coupled with the ONERA's CEDRE code to test the whole combustor's ignition. Its application to a combustion chamber of simple geometry has given the same trends as the experimental tests carried out on this combustor, confirming the prime importance of the spark-plug's location.

Future investigations will be devoted to improve the physical processes modelling, by introducing :

✔ a detailed chemical kinetics particularly in order to better evaluate the level of polluting emissions created,

✔ the group effects on vaporization and combustion rates for dense sprays.

NOMENCLATURE

Latin symbols

B_T [dimensionless]	Spalding number
Cp [J/(kg K)]	specific heat at constant pressure
D [m^2/s]	mass diffusion coefficient
k [m^2/s^2]	turbulent kinetic energy
l_m [m]	mixing length scale
$\dot{m}$ [kg/s]	drops vaporisation rate
Le [dimensionless]	Lewis number
n [m^{-3}]	drops density per volume unit
P [Pa]	pressure
Q_c [J/kg]	heat of combustion per mass unit of fuel burnt
r [m]	radial co-ordinate
r_k [m]	kernel's radius
R_{gp} [J/(kg K)]	perfect gas constant
t [s]	time
T[K]	temperature
W [kg/mol]	molecular weight
Y [dimensionless]	mass fraction
Z [dimensionless]	compressibility factor

Greek symbols

λ [W/(m K)]	thermal conductivity
ν [dimensionless]	stoechiometric coefficient
ρ [kg/m^3]	density
φ [dimensionless]	equivalence ratio
$\dot{\omega}$ [$mol/(m^3 s)$]	reaction rate

Subscripts

l	laminar
ref	reference condition
s	droplet's surface
t	turbulent
F	fuel
N_2	nitrogen
O	oxygen
P	products
0	initial condition
∞	outer condition

REFERENCES

1. A.Dreizler and al., Characterisation of a spark ignition system by planar laser-induced fluorescence of OH at high repetition rates and comparison with chemical kinetic calculations, *Appl. Phys*., vol. B70, pp. 287-294, 2000.

2. B.Abramzon and W.A. Sirignano, Droplet Vaporization Model for Spray Combustion Calculations, *Int. J. Heat Mass Transfer*, vol. 32, n°9, pp. 1605-1618, 1989.

3. C.K. Westbrook and F.L. Dryer, Simplified Reaction Mechanisms for the Oxidation of Hydrocarbon Fuels in Flames, *Combust. Sci. and Tech*., vol. 27, pp. 31-43, 1981.